

A Global Picture of Food Insecurity and Hunger

Matthew Cooper^{1,2,*}, Benjamin Müller^{2,3}, Carlo Cafiero⁴, Juan Carlos Laso^{2,5},
Wolfgang Fengler^{2,6}, and Homi Kharas^{2,7}

¹T.H. Chan School of Public Health, Harvard University

²The World Data Lab, Vienna, Austria

³Department of Economics, Vienna University of Economics and Business

⁴The Food and Agricultural Organization of the United Nations

⁵The International Institute for Applied Systems Analysis

⁶The World Bank

⁷The Brookings Institute

*Corresponding Author: mcooper@hsph.harvard.edu

October 26, 2020

Abstract

We modeled levels of food security at a subnational level from 2010 to 2030 using microdata from 77 countries collected by the FAO and Gallup World Poll for the Voices of the Hungry project. We find significant heterogeneity in levels of food security around the world, ranging from parts of the global north with less than 1% of the population food insecure to parts of the global south where as much as 3 out of 4 people are severely food insecure. Examining global temporal trends and accounting for the effects of the COVID-19 pandemic, we find that food insecurity has been increasing over the past several years, but under middle-of-the-road assumptions for development and population change, food insecurity will decline throughout the 2020s. This global decrease is largely driven by trends in South and East Asia, and some parts of the world, particularly sub-Saharan Africa, are projected to show increases in the prevalence of food insecurity throughout the next decade. This is the first global picture at a subnational level of the Food Insecurity Experience Scale, the food security metric most indicative of the lived experience of hunger.

1 Main

Food security is a critical component of human flourishing, which is why the second Sustainable Development Goal (SDG 2) is “Zero Hunger.” One of the indicators to track progress on the first target of this goal, to ensure access by everyone to safe, nutritious and sufficient food (SDG2.1), is the prevalence of moderate to severe food insecurity in the population based on the Food Insecurity Experience Scale, or FIES. The FIES was developed by FAO in 2013 as a global extension of pioneering work done on Latin America to develop a metric of food insecurity based on the perspective of people who experience it. Other indicators of food insecurity, such as FAO’s most commonly used estimate of undernourishment, are based on macro models of the mean and distribution of calories consumed per capita in a population. These do not capture the actual lived exposure of individuals to food shortages.

Because the FIES is based on responses to polls, the data is limited to 77 countries where the polls have been conducted and microdata has been vetted and released by the FAO. The current practice is to assign the regional average prevalence rate for countries without survey data in order to compile regional and global aggregates. This is not very satisfactory. In addition, because the FIES is a relatively new metric, it does not have a sufficiently long time series to

estimate trends with any degree of precision. To understand whether SDG 2 is being met, one needs to estimate food insecurity outcomes in 2030.

The contribution of this paper is to fill these two gaps of coverage and forecasts by developing a model of FIES outcomes that is based on covariates that are available for places where actual polling data is not available, and that can be forecast to 2030 to get a sense of what food insecurity at that time might look like. We also take advantage of the within-country spatial distribution of FIES reports to push the analysis beyond country level to a sub-national level, that is administratively once removed from the national level (Admin-1). To our knowledge, this is the first effort to model the FIES outcomes at that scale.

Food security has traditionally been difficult to measure, and this has led to incomplete or inaccurate pictures of global hunger. Metrics of macro-health, such as anthropometry and mortality rates are correlated broadly with food insecurity and have been used for many years to monitor human well-being [1, 2]. However, these metrics are confounded with other determinants of health such as infectious disease and are not meaningful at the scale of individuals or households [3]. Other proxies for food security, such as food availability estimated from crop yields [4], are also inadequate because they only make rough estimates of how accessible food is to the general population, and food insecurity can certainly occur in the absence of food availability decline [5]. Moreover, these metrics are very sensitive to incorrect estimates of crop yields and food reserves at a national scale. Thus, global estimates of hunger and food insecurity based on these metrics carry forward similar flaws.

As researchers began to focus on food insecurity at the individual and household level, household microdata collecting information on household finances and consumption became a common proxy for food security [6]. However, these efforts were criticized for being onerous, insufficiently comparable, as well as for ignoring subjective and experiential aspects of food security [7]. This led to the emergence of several indicators designed to be rapidly deployable, culturally cross-comparable, and based on the lived experience of food security [8]. These metrics include the Household Food Insecurity and Access Scale (HFIAS) [9]; the Coping Strategies Index (CSI) [10]; and the Household Hunger Scale (HHS) [11].

Drawing on the insights derived in designing and implementing these novel food security metrics, the FIES was developed by the Food and Agricultural Organization (FAO) of the UN [12] and quickly became a useful tool for understanding individual and household-level food insecurity [13]. The FIES is based on a survey of eight behaviors indicative of food insecurity and hunger over the previous year, such as skipping meals or worrying about having enough to eat. Using a Rash model [14], each individual in the survey is given a severity score that maximizes the likelihood of observing he responses given to the 8 questions asked in the survey. Once individuals are ranked in this fashion, thresholds for moderate and severe food insecurity are set that describe people's experiences, and the prevalences can be computed. A moderately food insecure adult has compromised on food quality and variety, as a result of lack of income, has been unsure about their ability to obtain food and has skipped meals or run out of food occasionally. A severely food insecure adult has run out of food and has gone an entire day without eating at times during the year.

Since 2014, in partnership with Gallup World Poll, the FAO has published surveys from around the world to estimate the prevalence of food insecurity using the FIES. Drawing on surveys from 77 countries, we used machine learning to estimate levels of food insecurity around the world at the subnational level. The model is then used to infer levels of food insecurity around the world at the subnational level and to forecast food insecurity to the year 2030.

2 Results

Globally, in the year 2020, we estimate that 829 million people are above the threshold for severe food insecurity, and an additional 1.5 billion people are above the threshold for moderate food insecurity (See Fig. 1). These numbers are higher than the estimates in the 2019 FAO State of Food Insecurity report, which estimated about 700 million severely food insecure people and an additional 1.31 billion people experiencing at least moderate food insecurity in 2018.

While the total number of people experiencing moderate and severe food insecurity held roughly constant for the 2010s and even increased in latter part of that decade, we predict that it will decline throughout the 2020s. However, this overall decline will not be uniform across the world. Our model expects that, in most of sub-Saharan Africa, moderate food insecurity will increase throughout the 2020s and severe food insecurity will plateau, although some countries, such as Kenya, Ethiopia, and Ghana, will see improvements. Food insecurity will fall in most other world regions, particularly South Asia and East Asia—the Pacific.

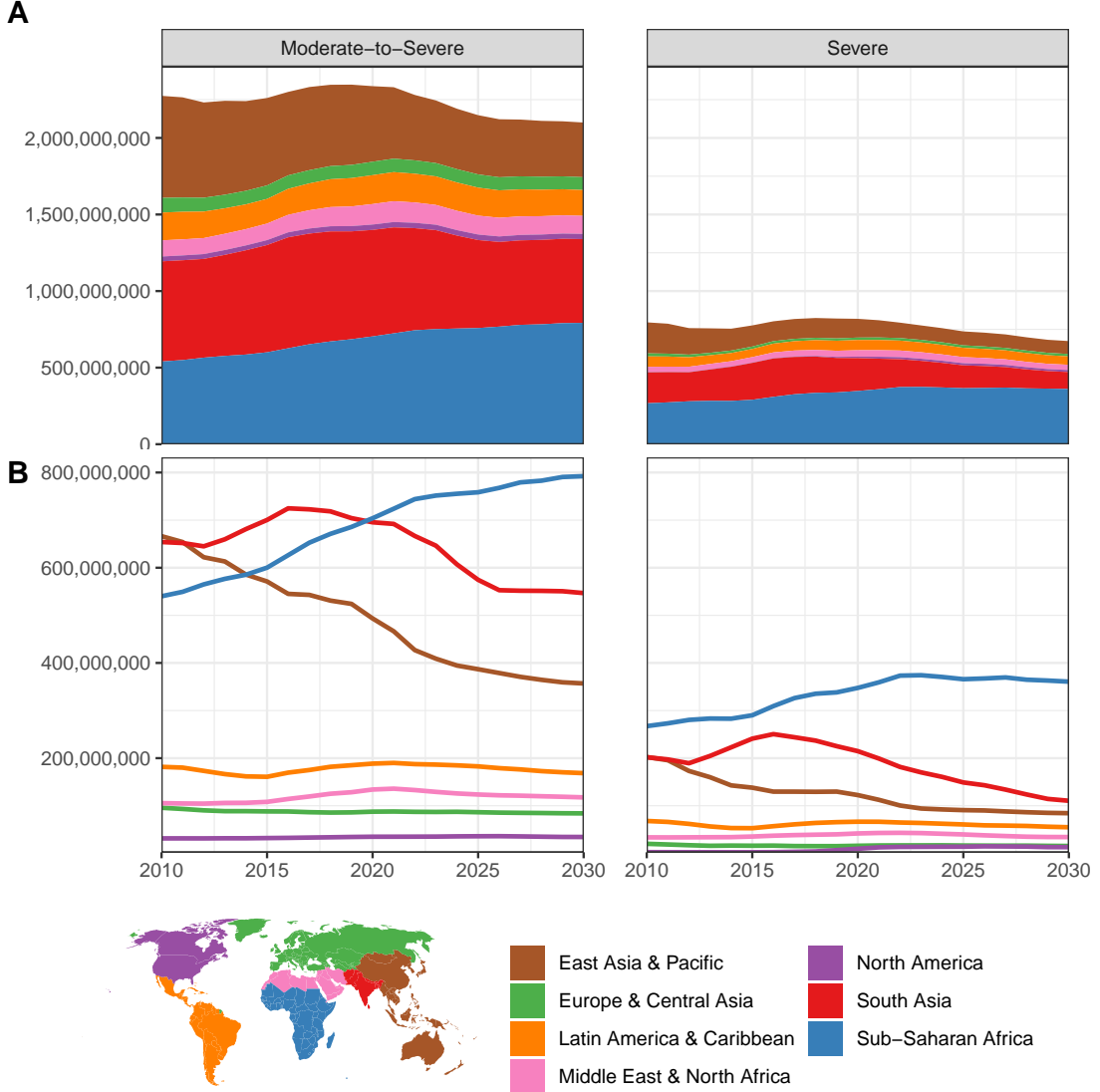
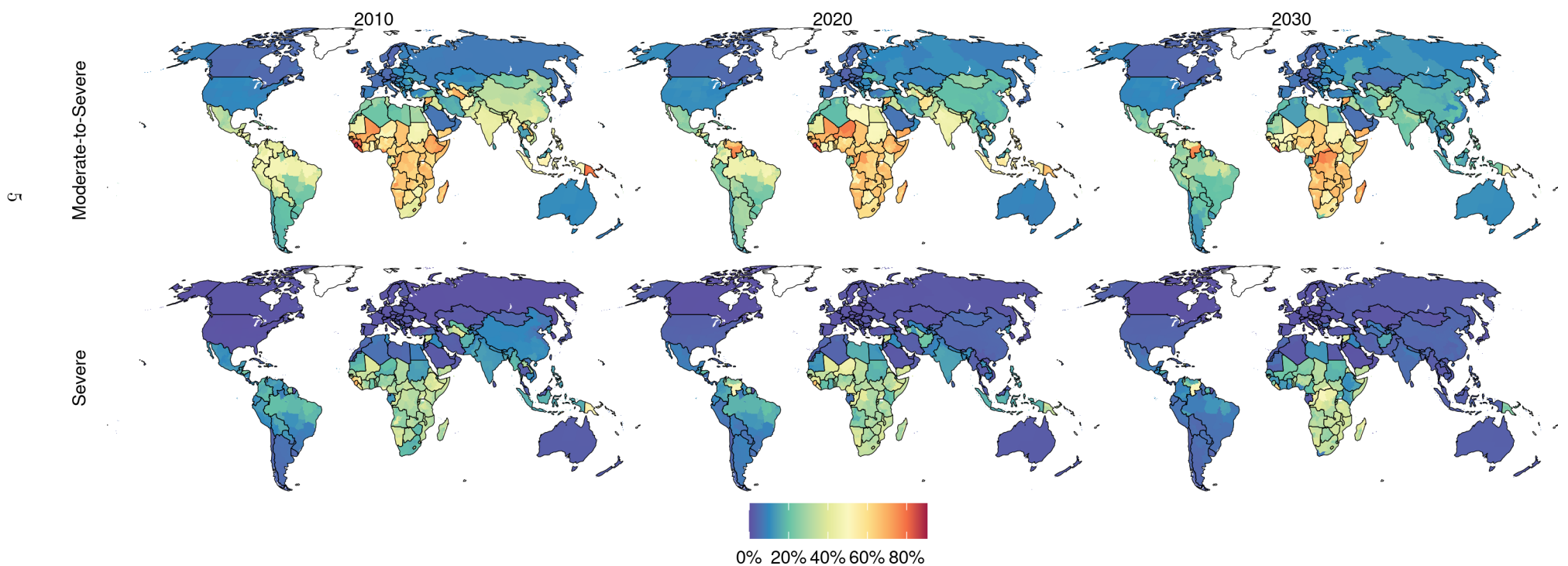


Figure 1: Number of people over the thresholds for moderate and severe food insecurity, by UN SDG regions over time, with a 3-year smoothing. Panel (A) shows the number of food insecure people with region totals stacked, to show global trends and totals over time. Panel (B) shows regional totals compared against each other over time.

We found substantial heterogeneity in the global distribution of severe food insecurity (See Fig. 2). For the year 2020, mainland sub-Saharan Africa is the continent with the highest rates of severe food insecurity, with at least 15% of people over the threshold for severe food insecurity in at least one subnational area in every country except Gabon and Equatorial Guinea. Outside of Africa, serious pockets of severe food insecurity also occur in Venezuela, Syria, Papua New Guinea, Yemen, and Afghanistan. In many large middle-income countries, severe food insecurity is also quite prevalent, with rates between 10-15% in areas like northern Brazil, many

central Asian and middle-eastern countries, and India and Indonesia.

The experience of at least moderate food insecurity is quite common in many parts of the world. In 2020, much of Africa, south and southeast Asia, and parts of Latin America had over 50% of the population living with moderate food insecurity. Even in countries widely considered to be developed, such as Australia, the United States, and parts of eastern and southern Europe, over 10% of the population is above the threshold for moderate food insecurity.



The results of this analysis can be further explored in more detail on the World Hunger Clock, including statistics for each subnational administrative area.

3 Discussion

This paper presents the first global estimates of the experience of food insecurity at a subnational level, with forecasts out to the year 2030. We found that, while food insecurity has been increasing and has likely worsened in 2020 with economic downturn associated with the novel coronavirus, our models predict that number of people who experience food insecurity globally will decrease throughout the 2020s, largely because of progress in south and east Asia. Nevertheless, many regions, most notably sub-Saharan Africa, are expected to see overall increases in the number of food insecure people.

While this is the first comprehensive projection of indicator 2.1.2 for SDG 2, projections for other indicators for that goal have been made. The most recent State of Food Insecurity (SOFI) report by the FAO projected indicator 2.1.1, the prevalence of undernourishment, and found that that, much like food insecurity, undernourishment had been increasing throughout the 2010s [15]. The SOFI report also modeled the prevalence of undernourishment in 2030 based on recent trends, giving more weight to recent years, and projected that undernourishment will increase by 2030 [15, Part 1, Page 11]. Using a similar method for modeling the prevalence of stunting (indicator 2.2.1), the SOFI reported that the rate of stunting would decrease by 2030 [15, Part 1, Page 30].

The fact that the SOFI expects increases in undernourishment while we predict decreases in food insecurity is likely due to our differing modeling approaches. While the SOFI report extrapolated recent trends in undernourishment, we modeled food insecurity based on projections of factors like GDP per capita, population, and the prevalence of stunting. We found that, in a random forest model, these predictors were very successful at predicting recent rates of both moderate-to-severe and severe food insecurity.

While we found that food insecurity will decrease overall by 2030, our model, which relies on middle-of-the-road assumptions, only expects the number of people experiencing moderate food insecurity to fall by 12% and the number of people experiencing severe food insecurity to fall by 20%. This still leaves billions of people eating less than they should and nearly half a billion people going entire days without eating a decade from now, a number that falls far short of the SDG 2 goal of “zero hunger.” Moreover, decreases in food insecurity as measured by the FIES do not necessarily mean there will be improvements in other significant challenges such as poor dietary quality, micronutrient deficiencies, or obesity. Thus, while expected trends in correlates of food security give cause for optimism, there is still significant work to be done in pursuit of SDG 2.

4 Methods

4.1 Disaggregation

The data on the FIES collected by Gallup records many individual-level attributes from the respondents, including age, gender, wealth quintile, and whether they live in an urban or rural area. Using national data on these variables, a standard weighting scheme is created for each individual, based on the ratio of population probabilities to sample probabilities of an individual with those characteristics being selected [16]. We used a similar methodology, except we calculated post-stratification weights at a subnational level. We used year-specific subnational estimates of population percentages by gender, age, urbanization, and, where available, wealth, and created a separate set of weights for each subnational area across all individuals. For age and gender, we used gridded data from WorldPop [17], for urbanization, we used spatially explicit estimates published by Jones and O'Neill [18], and for wealth we used data on household wealth quintiles from Demographic and Health Surveys [19], where available. This methodology rests

on the mild assumption that subnational differences in rates of food insecurity are more due to factors related to demographics, urbanization, and wealth than to other unobservable factors.

4.2 Covariates

We model subnational rates of severe and moderate-to-severe food insecurity as a function of several covariates related to human development, food security, health, infrastructure, income levels and distribution, and the environment (See Table 1). We aimed for covariates that had subnational spatial resolution and peer-reviewed projections available through the year 2030. For projections based on the Shared Socioeconomic Pathways (SSP) framework, we used the middle-of-the-road pathway, SSP2, and for climatological variables, we use forecasts based on Representative Concentration Pathway (RCP) 6.0.

Many of the variables required harmonizing subnational historic data with projections at the national level. This included mean years of schooling, GDP per capita, as well as for projections of population. We used observed trajectories in the historical distribution of variables among subnational areas within a country to estimate the future distribution of GDP, population, and schooling among subnational areas and disaggregate national-level future projections.

In cases of health variables that have shown long-term trends and represented a rate of occurrence in a population, including stunting, wasting, and malaria mortality rate, we estimate the Annualized Rate of Change (AROC) for each subnational area to model these variables for 2030. This involves taking the rate of change between each pair of years in the dataset, and then taking the mean rate of change over the period for which data is available, giving greater weight to more recent years. This method has been used to estimate rates of stunting and wasting in 2025 [20]; we simply use the same method to make forecasts to the year 2030.

For the climate variables temperature and precipitation, we combined historical observations with an ensemble of four bias-corrected simulations of the future climate from the Inter-Sectoral Impact Model Intercomparison Project (ISIMIP) [21].

Finally, we adjusted several variables to account for the effects of COVID-19, including GDP per capita using June 2020 estimates from the World Bank [22], stunting and wasting using August 2020 estimates published in *The Lancet* [23], as well as the poverty headcount index [24]. For a detailed overview of the steps involved in processing and preparing each covariate, see the Appendix.

Name	Source	Scale
Urban Percentage	[18]	Subnational
Stunting	[20]	Subnational
Wasting	[20]	Subnational
Mean Years of Schooling	[25, 26]	Subnational
GDP Per Capita	[25, 27]	Subnational
Gini Coefficient	[28]	National
Poverty Headcount Index	[24]	National
Water Scarcity	[29]	Subnational
Mean Annual Precipitation	[21, 30]	Subnational
Topographic Ruggedness	[31, 32]	Subnational
Mean Temperature	[21, 30]	Subnational
Malaria (<i>P. falciparum</i>) Mortality Rate	[33]	Subnational

Table 1: Covariates Included in Present-Day Analysis

4.3 Modeling

We fit two models for all subnational areas globally from 2010 to 2030: one for the percent of the population over the threshold for moderate food insecurity, and one for the percent of the population over the threshold for severe food insecurity. We used random forest regressions, as

this approach performs well in the presence of non-linearities and important interactions among predictor variables [34], while providing more model interpretability than other machine learning approaches [35]. A random forest regression involves generating a large number of decision trees, each under slightly different conditions and using different sub-samples of the data, and then aggregating the predictions of the decision trees.

Because the outcome variables in our models, the rate of moderate or severe food insecurity, is a bounded outcome, we first used a logistic transformation to extend the range from $[0, 1]$ to $(-\infty, \infty)$. Then, after estimating the model, we used the inverse logit to convert the unbounded model predictions to a rate between 0 and 1.

To get the best possible model performance, it is necessary to tune the hyperparameters, which control the process in which the random forest algorithm is run. Key hyperparameters include the number of decision trees to generate, the number of variables randomly selected as candidates for splitting a node, and the average number of observations in a leaf node. We calculated the Out-Of-Bag (OOB) error for different combinations of hyperparameters for the moderate-to-severe and severe models. By choosing the combinations of hyperparameters with the smallest OOB error we found the optimal combination for both models. We found that 5000 trees are more than sufficient for the error rates to converge (See Fig. S14).

We observed for the moderate as well as the severe model an in-sample mean squared error (MSE) between 0.002-0.005, with a R-squared (R^2) value of 0.999 (See Fig. S15). To test the out-of-sample prediction performance we used ten-fold cross-validation. First, we partitioned the data into ten equal sized subsamples. Once partitioned, we trained the RF regression models on nine subsamples and tested the models on the remaining one. This process gets repeated ten times, with each subsample being used once for testing. We then calculated the average MSE and R^2 over all ten out-of-sample predictions. Similarly to the in-sample model validation metrics, the average out-of-sample MSE is between 0.008-0.016, with an average R^2 of around 0.99 for both models (See Fig. S16). Besides using the full set of countries to validate the out-of-sample performance, we halved the sample size by excluding high-income countries (HIC) (according to the World Bank definition, REFERENCE NEEDED) and performed ten-fold cross-validation for this limited set of countries. We found that even when excluding HIC the average out-of-sample MSE is between 0.013-0.023, with an average R^2 of around 0.98 for both models.

After fitting the models, we examined the importance of the individual covariates in explaining rates of moderate and severe food insecurity. By training the models with all covariates and predicting rates with and without a individual variable we calculated the average prediction error of omitting that variable. Using the highest average prediction error we ranked the importance of the variables and found that for both, the moderate-to-severe and severe model, the Poverty Headcount Index, Stunting, GDP Per Capita and the Gini Coefficient are the most important variables for explaining differences in rates of moderate-to-severe and severe food insecurity (See Fig. S17).

For a detailed description, implementation and validation of the random forest models see the Supplemental Info.

5 Conclusion

References

- [1] Ruth R. Puffer and Carlos V. Serrano. *Patterns of Mortality in Childhood*. Washington, DC: World Heath Organization, 1973.
- [2] J P Habicht et al. “Height and weight standards for preschool children. How relevant are ethnic differences in growth potential?” In: *Lancet* 1.7858 (1974), p. 611. ISSN: 01406736. DOI: 10.1016/S0140-6736(74)92663-4.
- [3] Nandita Perumal, Diego G Bassani, and Daniel E Roth. “Use and Misuse of Stunting as a Measure of Child Health”. In: *The Journal of Nutrition* 148.3 (2018), pp. 311–315. ISSN: 0022-3166. DOI: 10.1093/jn/nxx064. URL: <https://academic.oup.com/jn/article-148/3/311/4930811>.

- [4] Simon Maxwell and Timothy R. Frankenberger. *Household Food Security: Concepts, Indicators, Measurements: A technical review*. 1992. DOI: 10.1016/0305-750X(92)90001-C. URL: http://www.ifad.org/hfs/tools/hfs/hfspub/hfs_toc.pdf.
- [5] Amartya Sen. *Poverty and famine: An essay on entitlement and deprivation*. 1983. ISBN: 0198284632. DOI: 10.1016/0147-5967(83)90075-6.
- [6] Lawrence Haddad, Eileen Kennedy, and Joan Sullivan. "Choice of indicators for food security and nutrition monitoring". In: *Food Policy* 19.3 (1994), pp. 329–343. ISSN: 03069192. DOI: 10.1016/0306-9192(94)90079-5.
- [7] Simon Maxwell. "Food security: A post-modern perspective". In: *Food Policy* 21.2 (1996), pp. 155–170. ISSN: 03069192. DOI: 10.1016/0306-9192(95)00074-7.
- [8] A. D. Jones et al. "What Are We Assessing When We Measure Food Security? A Compendium and Review of Current Metrics". In: *Advances in Nutrition: An International Review Journal* 4.5 (2013), pp. 481–505. ISSN: 2156-5376. DOI: 10.3945/an.113.004119. URL: <http://advances.nutrition.org/cgi/doi/10.3945/an.113.004119>.
- [9] J Coates, a Swindale, and P Bilinsky. "Household Food Insecurity Access Scale (HFIAS) for measurement of food access: indicator guide". In: *Washington, DC: Food and Nutrition Technical ... August (2007)*, Version 3. ISSN: 0717-6163. DOI: 10.1007/s13398-014-0173-7.2.
- [10] Daniel Maxwell et al. "Alternative food-security indicators: Revisiting the frequency and severity of 'coping strategies'". In: *Food Policy* (1999). ISSN: 03069192. DOI: 10.1016/S0306-9192(99)00051-2.
- [11] Terri Ballard. "Household Hunger Scale". In: *Measurement* (2011), p. 23. URL: http://www.fantaproject.org/downloads/pdfs/HHS_Indicator_Guide_Aug2011.pdf.
- [12] T Ballard, A Kepple, and C Cafiero. "The food insecurity experience scale: development of a global standard for monitoring hunger worldwide". In: *Technical Paper* (2013). ISSN: 0263-2241. DOI: 10.1016/j.measurement.2017.10.065.
- [13] Michael D Smith, Matthew P Rabbitt, and Alisha Coleman-Jensen. "Who are the world's food insecure? New evidence from the Food and Agriculture Organization's food insecurity experience scale". In: *World Development* 93 (2017), pp. 402–412.
- [14] Carlo Cafiero, Sara Viviani, and Mark Nord. "Food security measurement in a global context: The food insecurity experience scale". In: *Measurement: Journal of the International Measurement Confederation* (2018). ISSN: 02632241. DOI: 10.1016/j.measurement.2017.10.065.
- [15] FAO et al. *The State of Food Security and Nutrition in the World 2020. Transforming food systems for affordable healthy diets*. Rome, 2020. DOI: 10.4060/ca9692en.
- [16] Jelke Bethlehem. *Applied survey methods: A statistical perspective*. Vol. 558. John Wiley & Sons, 2009.
- [17] Andrew J Tatem. "WorldPop, open data for spatial demography". In: *Scientific Data* 4 (2017), p. 170004. ISSN: 2052-4463. DOI: 10.1038/sdata.2017.4.
- [18] B. Jones and B. C. O'Neill. "Spatially explicit global population scenarios consistent with the Shared Socioeconomic Pathways". In: *Environmental Research Letters* (2016). ISSN: 17489326. DOI: 10.1088/1748-9326/11/8/084003.
- [19] ICF. *Demographic and Health Surveys*. 2004-2017.
- [20] Local Burden of Disease Child Growth Failure Collaborators et al. "Mapping child growth failure across low-and middle-income countries". In: *Nature* 577.7789 (2020), p. 231.
- [21] Lila Warszawski et al. "The inter-sectoral impact model intercomparison project (ISI-MIP): project framework". In: *Proceedings of the National Academy of Sciences* 111.9 (2014), pp. 3228–3232.
- [22] Global Economic Prospects. "June 2020". In: *World Bank Group, Washington DC* (2020).

- [23] Derek Headey et al. “Impacts of COVID-19 on childhood malnutrition and nutrition-related mortality”. In: *The Lancet* 396.10250 (2020), pp. 519–521.
- [24] Jesús Crespo Cuaresma et al. “Will the Sustainable Development Goals be fulfilled? Assessing present and future global poverty”. In: *Palgrave Communications* 4.1 (2018), pp. 1–8.
- [25] Jeroen Smits and Iñaki Permanyer. “The subnational human development database”. In: *Scientific data* 6 (2019), p. 190038.
- [26] Samir KC and Wolfgang Lutz. “The human core of the shared socioeconomic pathways: Population scenarios by age, sex and level of education for all countries to 2100”. In: *Global Environmental Change* (2017). ISSN: 09593780. DOI: 10.1016/j.gloenvcha.2014.06.004.
- [27] Rob Dellink et al. “Long-term economic growth projections in the Shared Socioeconomic Pathways”. In: *Global Environmental Change* (2017). ISSN: 09593780. DOI: 10.1016/j.gloenvcha.2015.06.004.
- [28] Narasimha D. Rao et al. “Income inequality projections for the Shared Socioeconomic Pathways (SSPs)”. In: *Futures* (2019). ISSN: 00163287. DOI: 10.1016/j.futures.2018.07.001.
- [29] Peter Greve et al. “Global assessment of water challenges under uncertainty in water scarcity projections”. In: *Nature Sustainability* 1.9 (2018), pp. 486–494.
- [30] John T Abatzoglou et al. “TerraClimate, a high-resolution global dataset of monthly climate and climatic water balance from 1958–2015”. In: *Scientific data* 5 (2018), p. 170191.
- [31] USGS. *Global 30 Arc-Second Elevation (GTOPO30)*. 1996. DOI: <https://lta.cr.usgs.gov/GTOPO30>.
- [32] S J Riley, S D DeGloria, and R Elliot. “A Terrain Ruggedness Index that Quantifies Topographic Heterogeneity”. In: *Intermountain Journal of Sciences* (1999). DOI: citeulike-article-id:8858430.
- [33] Daniel J. Weiss et al. “Mapping the global prevalence, incidence, and mortality of Plasmodium falciparum, 2000–17: a spatial and temporal modelling study”. In: *The Lancet* (2019). ISSN: 1474547X. DOI: 10.1016/S0140-6736(19)31097-9.
- [34] Trevor Hastie, Robert Tibshirani, and Jerome Friedman. *The elements of statistical learning: data mining, inference, and prediction*. Springer Science & Business Media, 2009.
- [35] Hemant Ishwaran et al. “Variable importance in binary regression trees and forests”. In: *Electronic Journal of Statistics* 1 (2007), pp. 519–537.
- [36] H Ishwaran and UB Kogalur. “randomForestSRC: Fast unified random forests for survival, regression, and classification (RF-SRC)”. In: *R Package Version* 2.1 (2019).
- [37] Leo Breiman. “Random forests”. In: *Machine learning* 45.1 (2001), pp. 5–32.

Supplemental Info

S1 Component Questions of the FIES

1. During the last 12 MONTHS, was there a time when you were worried you would not have enough food to eat because of a lack of money or other resources?
2. Still thinking about the last 12 MONTHS, was there a time when you were unable to eat healthy and nutritious food because of a lack of money or other resources?
3. Was there a time when you ate only a few kinds of foods because of a lack of money or other resources?
4. Was there a time when you had to skip a meal because there was not enough money or other resources to get food?

5. Still thinking about the last 12 MONTHS, was there a time when you ate less than you thought you should because of a lack of money or other resources?
6. Was there a time when your household ran out of food because of a lack of money or other resources?
7. Was there a time when you were hungry but did not eat because there was not enough money or other resources for food?
8. During the last 12 MONTHS, was there a time when you went without eating for a whole day because of a lack of money or other resources?

S2 Predicting Covariates Into the Future

S2.1 Annualized Rate of Change

For many of our covariates, to extrapolate recent trends to the future, it is necessary to draw on annualized rates of change, which are then used to anticipate the rate of future change. This method can be used for any variable that is a fraction or a rate. We use this method to estimate future rates of stunting, wasting, and malaria mortality, as well as to model future subnational shares of GDP and population. Thus, we give an overview of the methodology here.

First, for each subnational area, a , the rate of change (ROC) is calculated between each pair of adjacent years, y , based on a value, p , such that $0 < p < 1$, available for each year.

$$\text{ROC}_{a,y} = \text{logit} \left(\frac{p_{a,y}}{p_{a,y-1}} \right) \quad (1)$$

Then, each ROC is weighted to give more weight to recent years, such that weight W at year y is. For a dataset with observations for 2010 to 2017, that would be:

$$W_y = \frac{y - 2010}{\sum_{y=2010}^{2017} y - 2010} \quad (2)$$

Then, the annualized rate of change (AROC) is calculated as:

$$\text{AROC}_a = \text{logit} \left(\sum_{y=2010}^{2017} W_y \times \text{ROC}_{a,y} \right) \quad (3)$$

Finally, the projections, Proj, for each year from 2018 to 2030 are given as:

$$\text{Proj}_{a,y} = \text{logit}^{-1}(\text{logit}(p_{a,2017}) + \text{AROC}_a \times (y - 2017)) \quad (4)$$

For cases where we are modeling shares of a whole, for example when modeling subnational shares of population or GDP, we then re-scale the shares to ensure they total to 1.

S2.2 Population

Although population is not a covariate in our random forest model, it is an important precursor to other covariates, such as GDP per capita, and future estimates of population are also necessary to convert modeled future rates of food insecurity into total headcounts of food insecurity. Thus, in addition to our other covariates, we also modeled population into the future.

We do this by combining historic subnational data from the Subnational Development Database [25] with national level population estimates for the 21st century [26]. To account for within-country trends and changes in population distribution, we use the AROC method outlined in equations 1 - 4 to project each subnational areas share of national population totals. We then disaggregate the national totals given by KC et al. to estimate future subnational populations.

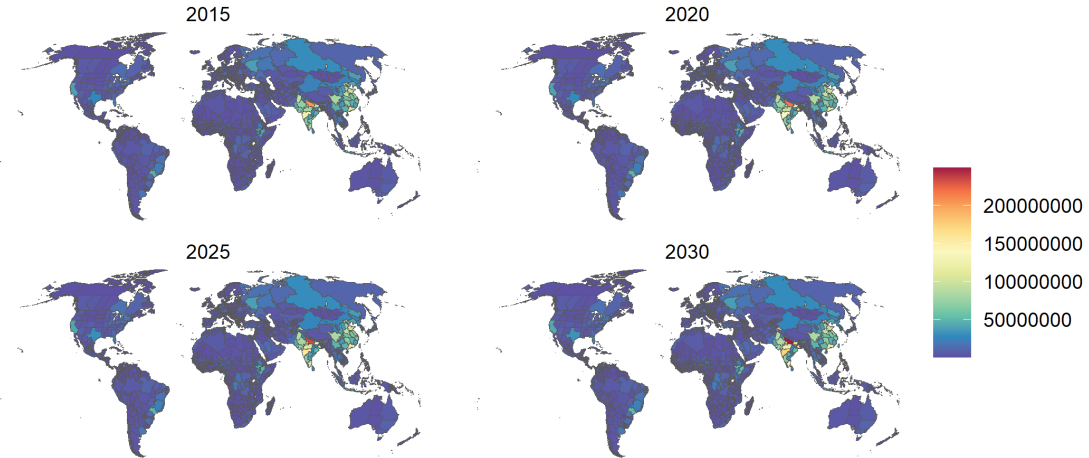


Figure S1: Population

S2.3 Urban Percentage

We drew our historic and future estimates of urbanization entirely from Jones and O’Neill, published in *Environmental Research Letters* [18], who modeled spatially explicit scenarios of urbanization consistent with the Shared Socioeconomic Pathways. As with our other covariates, we used estimates for SSP2, the middle-of-the-road scenario. Because definitions of “urban” and “rural” vary significantly across datasets, using one dataset that is entirely consistent within itself was an important consideration.

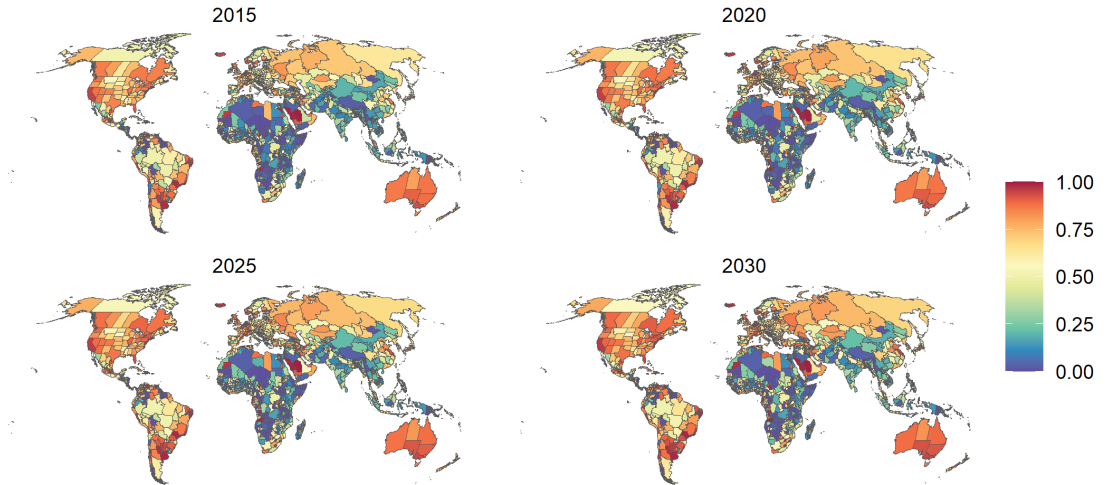


Figure S2: Percentage of people living in urban areas.

S2.4 Wasting

To estimate the prevalence of wasting for each administrative area in our dataset, we used data from the Local Burden of Disease project published in *Nature* [20]. For the years 2010 to 2017, we simply took the mean rate of wasting in each administrative area from the dataset. Higher-income countries that were not included in the dataset were modeled as having a rate of 0 wasting. We then modeled wasting for the years 2018-2030 using the AROC method, which the Local Burden of Disease group similarly used to estimate wasting for the year 2025 [20].

To account for the effects of the novel coronavirus on global rates of wasting, we assumed that long-term trends and rates of wasting would hold steady, but that they increase globally by 14.3% in 2020, based on estimates published in *The Lancet* [23]. We model this impact as uniform across all countries where wasting occurs. Then we model the rate of wasting in each administrative area in 2021 as being the mean of the rate in 2020 that accounts for the shock and the previously modeled rate for 2022.

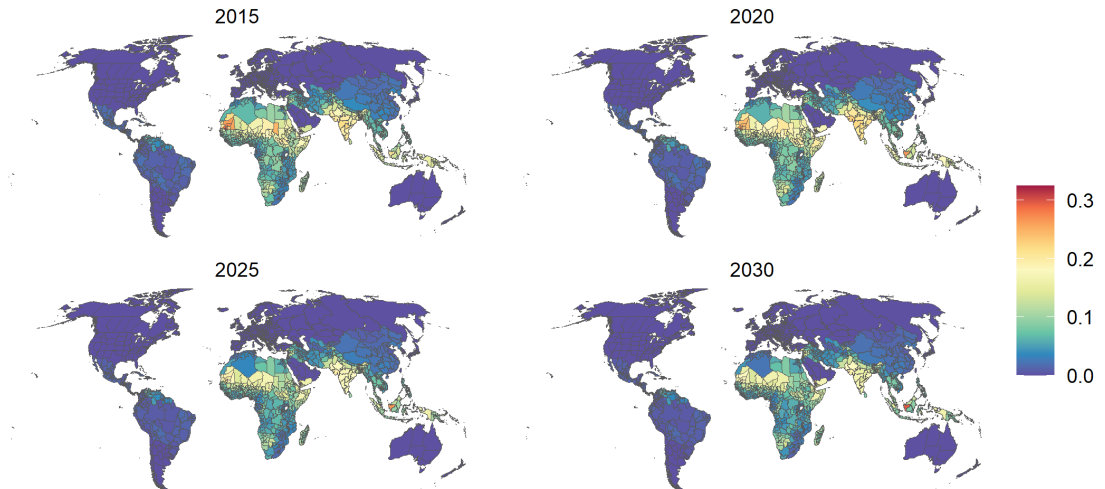


Figure S3: Prevalence of wasting.

S2.5 Stunting

We model stunting using the same methodology we use to summarize and model wasting, because the Local Burden of Disease dataset that we draw on for wasting also includes stunting. We also included the 14.3% increase in prevalence for the year 2020 that was estimated for wasting [23], even though stunting is a long-term consequence of malnutrition and will likely not be as readily observable in a population as wasting would be. However, we use stunting in our model not as a cause of food insecurity, but rather as a proxy for chronic conditions of hunger, which are exacerbated by the coronavirus pandemic. Thus, estimating an impact of the coronavirus shock on stunting is appropriate for our model.

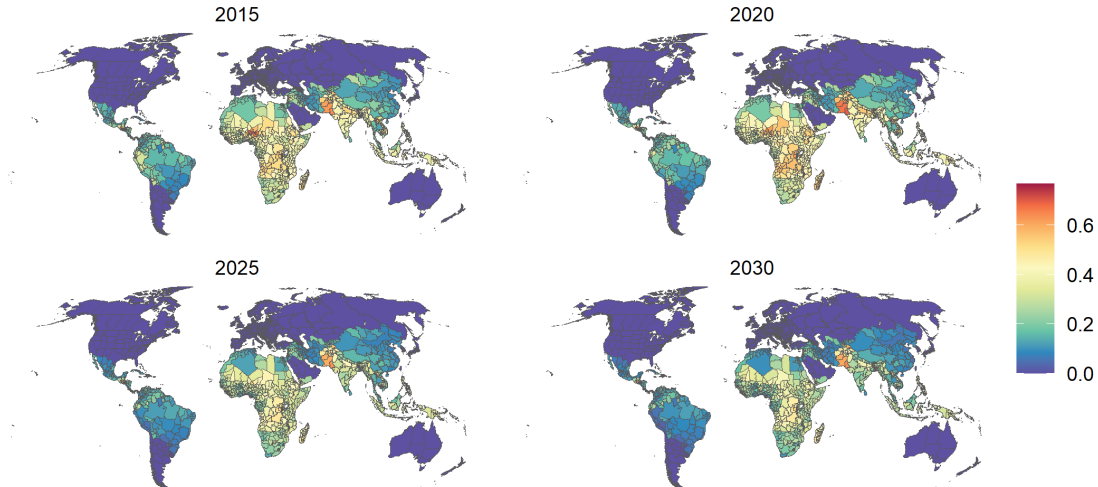


Figure S4: Prevalence of stunting.

S2.6 GDP Per Capita

We estimate global subnational GDP per capita using historic subnational estimates of Gross National Income (GNI) from the Subnational Human Development Database [25] and forecasts of national GDP within the SSP framework from Dellink et al. [27]. We first use data from the World Bank to estimate the mean country-level ratio of GNI to GDP and adjust the subnational estimates of GNI according to that country-specific ratio. We then calculate each subnational area's share of country GDP, and then use the AROC method to estimate each subnational area's share of total country GDP. Based on these trajectories in each subnational areas share of total country GDP, we estimate what each subnational area's share of GDP will be for each year from 2019 to 2030. We divide that share of GDP by the population of the administrative area, which we had previously estimated. Thus, national GDP totals are consistent with the projections of Dellink et al., but are disaggregated according to the historic patters of GDP share in the Subnational Human Development Database.

Finally, we used estimates of country-level changes in GDP growth for the years 2020 and 2021 to account for the impact of the coronavirus [22]. We then model GDP as resuming its previous growth trajectory based on previously-estimated growth rates from 2022-2030, but growing from an estimate for 2021 that includes the coronavirus shock.

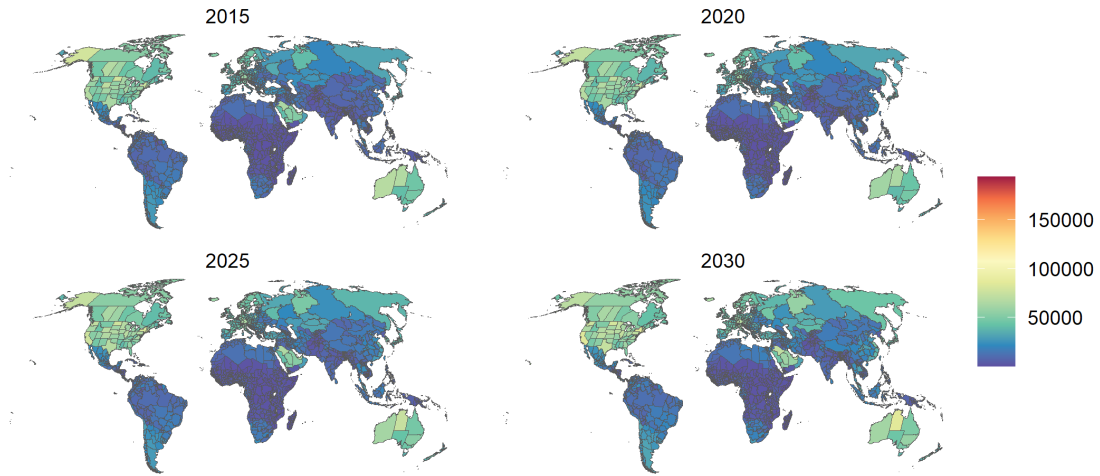


Figure S5: GDP per capita.

S2.7 Mean Years of Schooling

We estimate global subnational mean years of schooling using historic subnational estimates from the Subnational Human Development Database [25] and forecasts of national mean years of schooling from KC et al. [26]. Using the historic subnational data, we estimate each subnational administrative area's difference in years of schooling from the national mean, and use this value to disaggregate the future projections to a subnational level.

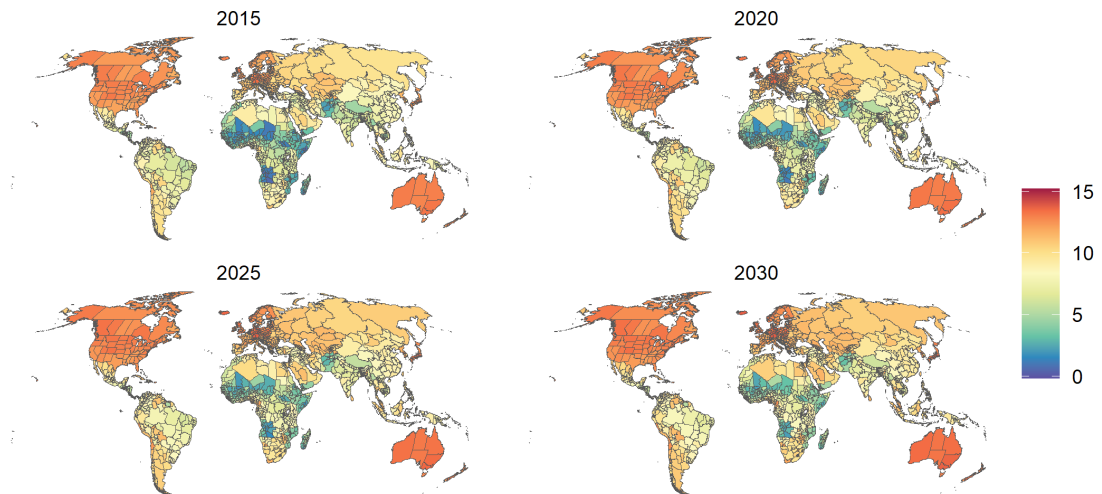


Figure S6: Mean years of schooling.

S2.8 Gini Coefficient

We use estimates of national income inequality from Rao et al. [28]. These estimates include all years in our analysis, and are not disaggregated to a subnational level.

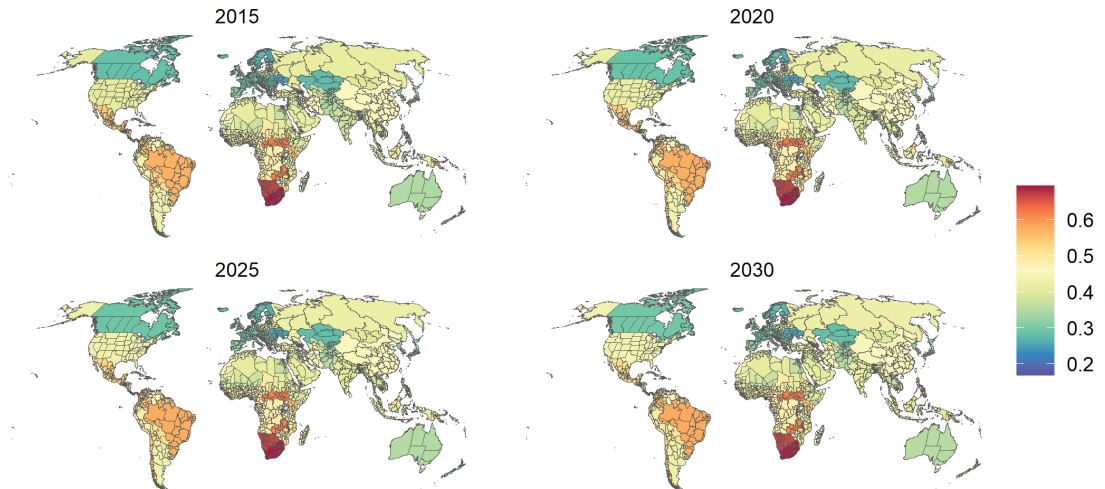


Figure S7: Gini Coefficient

S2.9 Poverty Headcount Index

We used estimates of the Poverty Headcount Index for the recent past and future from the World Poverty Clock by the World Data Lab [24], updated to include the impact of the coronavirus. In our model we include national level poverty rates at a threshold of \$1.90 which is defined as *extreme* poverty. By using the concept of parameterized Lorenz curves in combination with mean income/consumption and population projections future poverty rates are calculated. For more details on the methodology and information on global and country level poverty check the website worldpoverty.io.

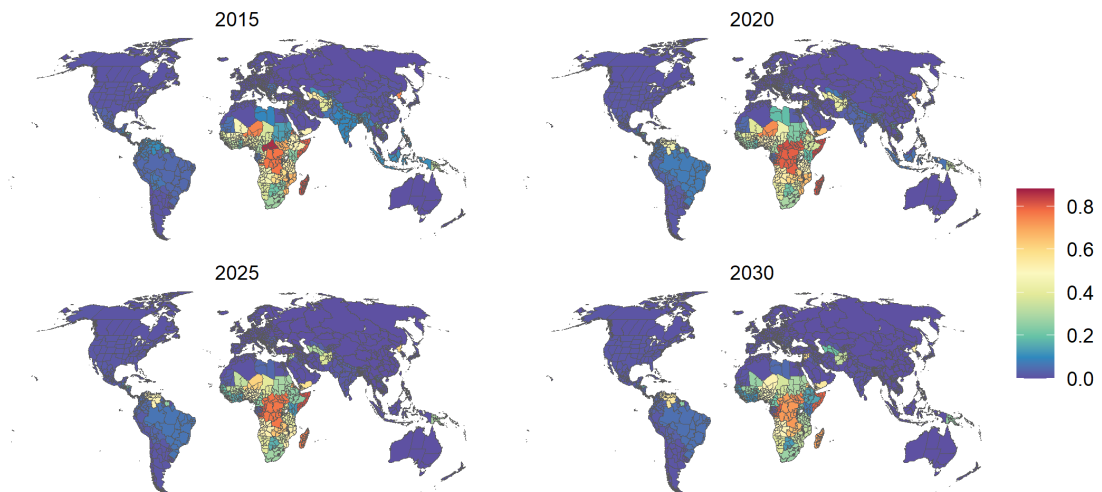


Figure S8: Poverty Headcount Index

S2.10 Water Scarcity Share

We used the water scarcity index (WSI) developed by [29]. The index represents the ratio of the decadal averages in water demand to water supply and it assesses changes in water scarcity on a 0.5 by 0.5 degree global grid. Based on this index, we estimate the share of people living in areas with less than 1000m^3 of water available per capita per year. The WSI has been used already to build the water scarcity clock. For more information visit worldwater.io.

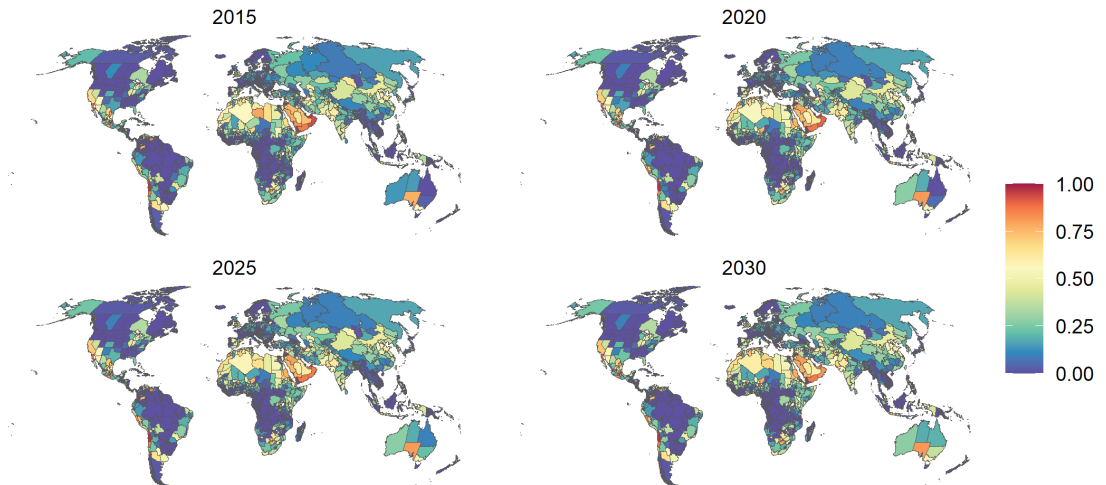


Figure S9: Water Scarcity Share

S2.11 Mean Annual Precipitation

For mean annual precipitation, we use data for the years 2010 to 2019 from the TerraClimate dataset [30], summarized to each subnational area. For data for the years 2020-2030, we use models from the Inter-Sectoral Model Intercomparison Project [21]. Specifically, we use an ensemble of bias-corrected projections under representative concentration pathway (RCP) 6.0, taking the mean of the ensemble.

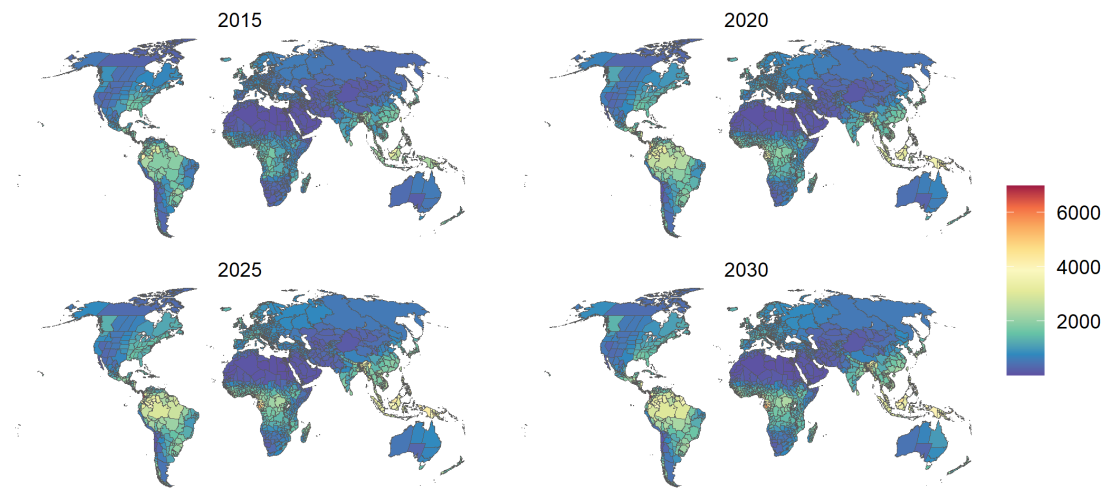


Figure S10: Mean annual precipitation

S2.12 Mean Temperature

For mean temperature, we used the same datasets that we'd used for precipitation, as each of those datasets included both temperature in addition to precipitation.

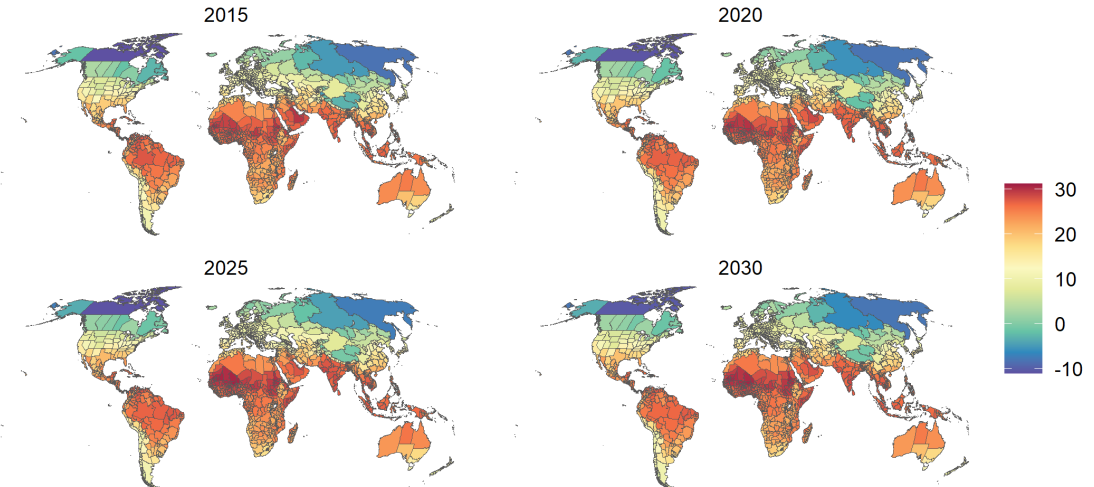


Figure S11: Mean temperature (Celsius)

S2.13 Topographic Ruggedness

As a measure of accessibility, we include the mean topographic ruggedness of each subnational area. We first used a gridded dataset of elevation from the USGS [31] and calculated the index at each grid cell using the methodology from Riley et al. [32]. We then summarized the values of all the grid cells within each administrative area. Because this variable does not change over time, it is constant across all years in the model.

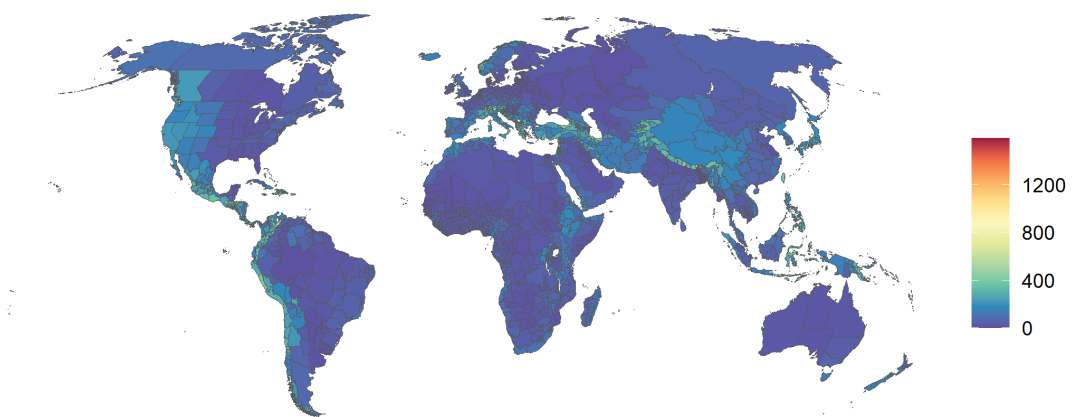


Figure S12: Topographic ruggedness

S2.14 Malaria (*P. falciparum*) Mortality Rate

We used data from *The Lancet* to estimate the mortality (deaths per 100,000 population per year) due to Malaria [33], taking the average pixel values within each subnational administrative area. We then estimated future malaria mortality based on AROC method.

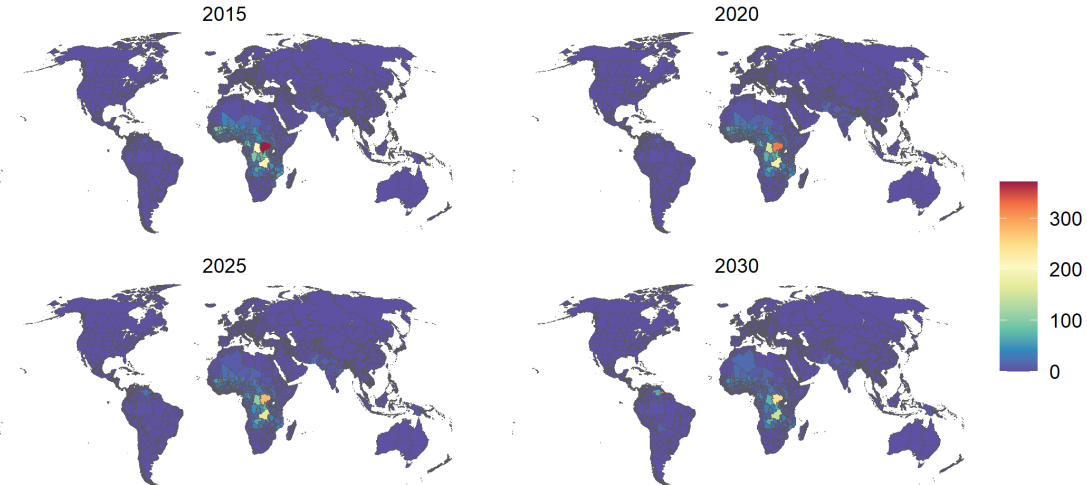


Figure S13: Rate of mortality due to *P. falciparum* Malaria

S3 Description, Implementation and Validation of the RF regression model

The RF regression is a machine learning method based on the creation of a large number of decision trees. By taking an ensemble of decision tree models, random forests introduce more variance and balance out the bias that is common to single decision trees [**friedman2001elements**]. For each of the decision trees in a random forest model, observations are selected at random with replacement, a method known as bootstrap aggregating, or bagging, and features are also selected at random.

For implementation we use the R-package `randomForestSRC` by Ishwaran and Kogalur [36]. Specifically, we apply the functions `tune.rfsrc()` to find the optimal combination of hyperparameters and the function `rfsrc()` to perform the RF regression models. After predicting rates of moderate-to-severe and severe food insecurity we plot the modeled vs. observed rates and calculated the MSE and R^2 (See Fig. S15 and Fig. S16) for both models. Additionally, we use the function `vimp()` to gain insights into the development of the error rates with increasing numbers of trees (See Fig. S14) and the importance of individual variables (See Fig. S17).

To ensure that predicted rates are bounded by 0 and 1 we conduct a logit transformation of the dependent variable and inverse logit transformation of the predictions.

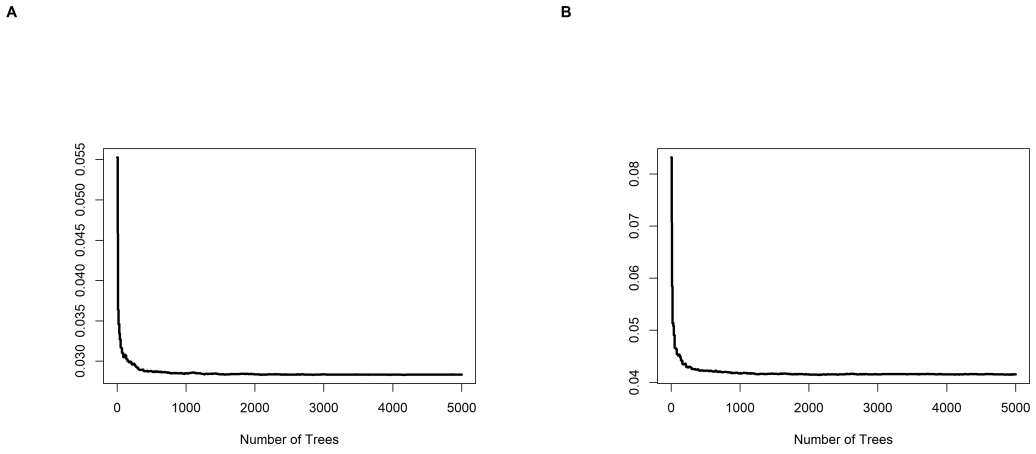


Figure S14: Error Rate of the RF regression model. Panel (A) shows the Moderate-to-Severe model and Panel (B) shows the Severe model.

In addition to the parameter that describes the number of trees to be created, two other important hyperparameters must be tuned. In the function `tune.rfsrc()` these parameters are called `mtry` and `nodesize`. `mtry` describes the number of variables randomly selected as candidates for splitting a node and `nodesize` describes the average number of observations in a leaf node. The optimal pair of hyperparameters is found by trying different combinations and choosing the one with the smallest out-of-bag (OOB) error.

The function `tune.rfsrc()` does exactly that and returns optimal values for `mtry` and `nodesize`. We applied this function on the both, the moderate-to-severe and the severe model. For the moderate-to-severe model the optimal combination is `mtry = 12` and `nodesize = 1` and for the severe model we found `mtry = 10` and `nodesize = 2` to be optimal.

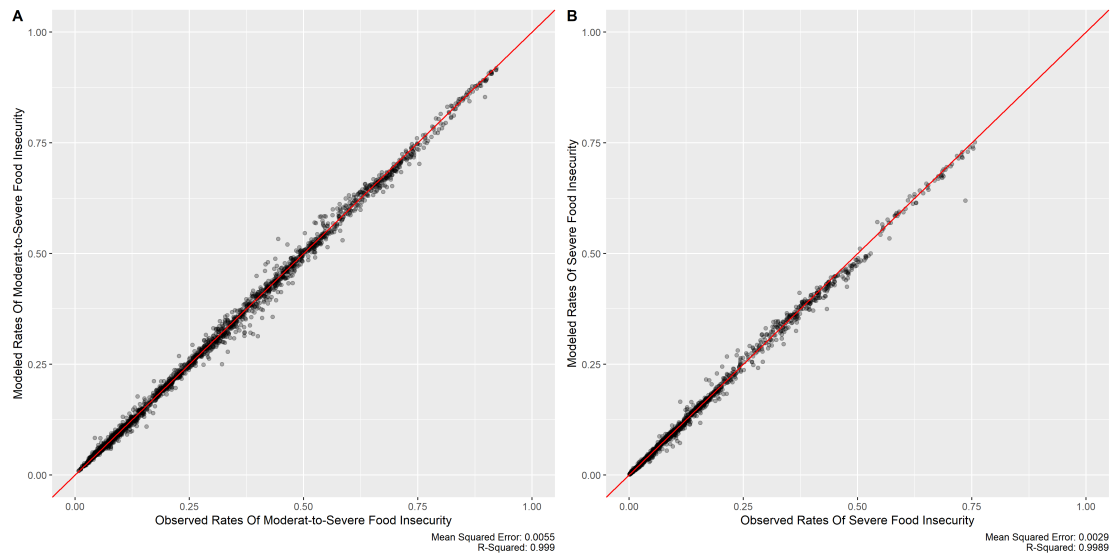


Figure S15: In-Sample Fit of the RF regression model. Panel (A) shows the Moderate-to-Severe model and Panel (B) shows the Severe model.

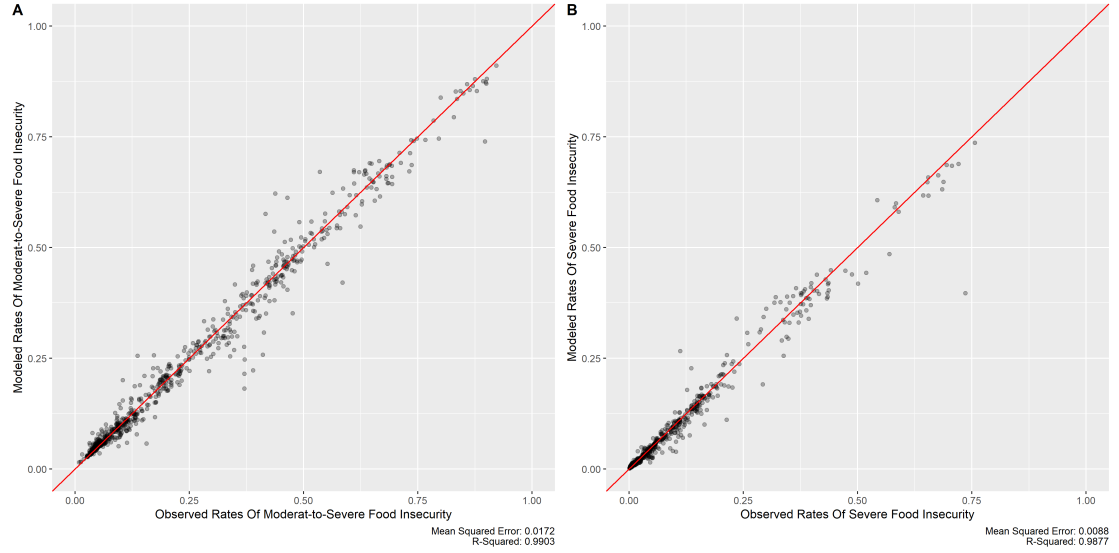


Figure S16: Out-Of-Sample Fit of the RF regression model with 75% training set and 25% test set. Panel (A) shows the Moderate-to-Severe model and Panel (B) shows the Severe model.

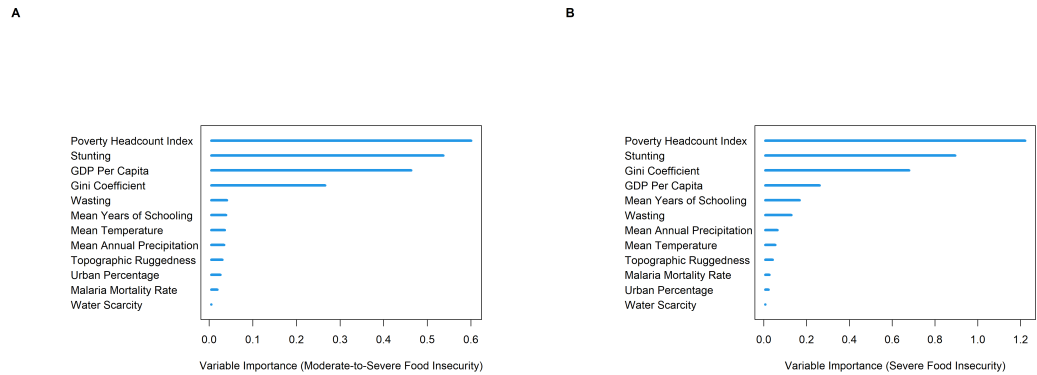


Figure S17: Variable Importance of the RF regression model. Panel (A) shows the Moderate-to-Severe model and Panel (B) shows the Severe model.

Lastly we asses the importance of individual variables. This is based on the Breiman-Culter permutation variable importance information [37]. This involved comparing the prediction error on the OOB data to the prediction error of OOB cases where the x-variable x is randomly permuted. The importance of an individual variable is thus the mean difference between the perturbed and unperturbed error rate, across all trees.